Solvothermal Syntheses, Crystal Structures of Two New Thioantimonates(III) of the $Mn_2(L)Sb_2S_5$ Family with L = Diethylenetriamine and *N*-Methyl-1,3-Diaminopropane and a Study of the Magnetic Properties of Four Compounds of the Series

L. Engelke[a], R. Stähler[a], M. Schur[a], C. Näther[a], W. Bensch[a], R. Pöttgen[b], and M. H. Möller[b]

[a] Institut für Anorganische Chemie, Olshausenstraße 40, D-24118 Kiel, Germany
[b] Institut für Anorganische und Analytische Chemie, Wilhelm Klemm Straße 8, D-48149 Münster, Germany

Reprint requests to Prof. Dr. Wolfgang Bensch. Fax: +49(0)431 880 1520.
E-mail: wbensch@ac.uni-kiel.de

Z. Naturforsch. **59b,** 869 – 876 (2004); received March 26, 2004

The two new compounds $Mn_2(L)Sb_2S_5$ (L = diethylenetriamine = DIEN, N-methyl-1,3-diaminopropane = MDAP) were prepared under solvothermal conditions using the elements as starting materials. Both compounds crystallise in the monoclinic space group $P2_1/c$ with the lattice parameters $a = 10.669(7)$, $b = 12.805(2)$, $c = 12.072(1)$ Å, $\beta = 115.786(7)^\circ$, $V = 1485.1(4)$ Å^3 for L = DIEN and $a = 10.1859(7)$, $b = 12.7806(6)$, $c = 12.1256(8)$ Å, $\beta = 110.173(8)^\circ$, $V = 1481.7(2)$ Å^3 for L = MDAP and $Z = 4$. The primary building units are SbS_3 pyramids, MnS_6 and MnS_4N_2 distorted octahedra. These primary building blocks are interconnected to form $Mn_2Sb_2S_4$ hetero-cubane units. The hetero-cubanes share common corners, edges and faces thus forming a second hetero-cubane. These secondary building units are joined to form layers within the (100) plane. The connection mode yields ellipsoidal pores within the layers. The amines are exclusively bound to one of the two crystallographically independent Mn^{2+} cations and they point into the pores and between the layers separating the layers from each other. The interlayer separation and the size of the pores depend on the sterical requirements of the amine incorporated into the network. A pronounced distortion of the MnS_4N_2 octahedron results from a significant elongation of one Mn-S distance from 2.866 Å (L = methylamine, MA) to 3.185 Å for L = MDAP. The magnetic susceptibility curves are typical for low-dimensional antiferromagnetic materials and the large negative values for the Weiss constant Θ indicate strong antiferromagnetic exchange interactions. The magnetic properties are significantly influenced by the change of the Mn-S bonds introduced by the different amines. The compounds decompose at elevated temperatures with a two step reaction for L = MA and ethylenediamine and in a one step reaction for the bidentate acting amine molecules.

Key words: Solvothermal Synthesis, Thioantimonates, Crystal Structures, Magnetic Properties, Thermal Decomposition

Introduction

A large number of fascinating thioantimonates(III) exhibiting a broad variety of structural features was synthesised and characterised by Schäfer and coworkers [1 – 10]. During the last decade many new compounds based on $Sb_xS_y^{z-}$ moieties were prepared under solvothermal conditions [11-38]. The Sb(III) atom has coordination numbers ranging from 3 to 6 yielding a rich structural diversity: isolated units, one-dimensional chains, two-dimensional layered arrangements as well as three-dimensional networks are observed. It was demonstrated by Wang and Liebau that the high coordination flexibility of the Sb(III) atom is due to the stereochemically active $6s^2$ lone pair [39]. It is of interest that until now only very few thioantimonate(III) compounds were synthesised under solvothermal conditions that contain a transition metal incorporated into the anionic thioantimonate(III) framework [11 – 16, 22 – 24, 28 – 30, 38].

The first compounds composed of polymeric transition metal thioantimonates(III) with general composition $Mn_2(L)Sb_2S_5$ with L = methylamine (MA), ethylamine (EA) and diaminopropane (DAP) were prepared and characterised a few years ago [15, 30]. A comparison of the structural details of the 3 compounds

Table 1. Details of the data collections and some refinement results for $Mn_2(MDAP)Sb_2S_5$ and $Mn_2(DIEN)Sb_2S_5$.

	$Mn_2(MDAP)Sb_2S_5$	$Mn_2(DIEN)Sb_2S_5$
a [Å]	10.669(7)	10.1859(7)
b [Å]	12.805(2)	12.7806(6)
c [Å]	12.072(1)	12.1256(8)
β [°]	115.786(7)	110.173(8)
V [Å^3]	1485.1(4)	1481.7(2)
Temperature [K]	293	293
Z	4	4
μ [mm^{-1}]	5.934	5.953
Formula weight [g/mol]	601.84	616.85
Space group	$P2_1/c$	$P2_1/c$
Density (calc) [g/cm^3]	2.692	2.765
Diffractometer	PHILIPS PW1100	STOE IPDS
2θ-Range	3°–54°	4.6°–60.8°
Data collected	3708	11206
Unique data	3241	3206
Data ($F_0 > 4\sigma(F_0)$)	2277	2811
No. refined parameters	138	146
δF [e/Å^3]	$0.76/-0.79$	$0.71/-0.75$
y, z[a]	0.0308/1.65	0.0425/2.11
$R1(F_0 > 4(F_0))$	0.0310	0.0285
$R1$ (all data)	0.0720	0.0344
$wR2(F_0 > 4\sigma(F_0))$	0.0654	0.0742
$wR2$ (all data)	0.1115	0.0769
Goodness of fit	1.054	1.038

[a] $w = 1/[\sigma^2(F_o^2) + (y \cdot P)^2 + z \cdot P]$; $P = (\mathrm{Max}(F_o^2, 0) + 2 \cdot F_c^2)/3$.

Table 2. Atomic coordinates for $Mn_2(MDAP)Sb_2S_5$. Estimated standard deviations are given in parentheses. All atoms occupy the Wyckoff site 4e.

Atom	x	y	z	U_{eq} [Å^2]
Sb(1)	0.3300(1)	0.4835(1)	0.2143(1)	0.022(1)
Sb(2)	0.3219(1)	0.7843(1)	0.2152(1)	0.023(1)
Mn(1)	0.6530(1)	0.6923(1)	0.2550(1)	0.027(1)
Mn(2)	0.4915(1)	0.6433(1)	0.4987(1)	0.024(1)
S(1)	0.5529(2)	0.7928(1)	0.3833(1)	0.022(1)
S(2)	0.5670(2)	0.4998(1)	0.3742(1)	0.023(1)
S(3)	0.2476(2)	0.6305(1)	0.3025(1)	0.023(1)
S(4)	0.7355(2)	0.8503(1)	0.1762(1)	0.024(1)
S(5)	0.3954(2)	0.6957(1)	0.0793(1)	0.024(1)
N(1)	0.6924(6)	0.5612(4)	0.1546(5)	0.031(1)
N(2)	0.8600(5)	0.6613(4)	0.4160(4)	0.028(1)
C(2)	0.9674(6)	0.6230(5)	0.3796(6)	0.033(1)
C(1)	0.8330(8)	0.5248(6)	0.1773(6)	0.038(2)
C(3)	0.9320(7)	0.5194(5)	0.3125(6)	0.036(2)
C(4)	0.9124(7)	0.7530(6)	0.4978(6)	0.040(2)

The U_{eq} is defined as one third of the trace of the orthogonalised U_{ij} tensor.

gave evidences that the $Mn_2Sb_2S_5$ network is flexible enough to account for the sterical demands of different organic ligands. It should be noted here that the compound $Mn_2(EN)Sb_2S_5$ (EN = ethylenediamine) [16] exhibits a significantly different network topology as compared to the above mentioned compounds.

In further investigations a variety of multidentate amines with different sizes and shapes were applied in the syntheses to elucidate the geometrical limits of the $Mn_2Sb_2S_5$ framework. During these studies we have isolated two new members of the $Mn_2(L)Sb_2S_5$ series. Here we report the results about the syntheses, structural investigations as well as thermal stability of the new compounds $Mn_2(C_4H_{12}N_2)Sb_2S_5$ and $Mn_2(C_4H_{13}N_3)Sb_2S_5$ containing *N*-Metyl-1,3-diaminopropane (MDAP) and Diethylenetriamine (DIEN) ligands. The influence of the different amines onto the structure and the geometry of the framework for the five known $Mn_2(L)Sb_2S_5$ compounds is discussed. In addition, the magnetic properties of the four compounds with L = MA, DIEN, DAP and MDAP were investigated and the differences are discussed on the basis of the structural changes.

Experimental Section

Syntheses

The two new manganese thioantimonate(III) compounds were prepared under hydrothermal conditions. A stoichiometric mixture of elemental Mn (0.11 g, 2 mmol), Sb (0.244 g, 2 mmol) and S (0.16 g, 5 mmol) was mixed with 5 ml of an 50% aqueous solution of the respective amine in a teflon lined steel autoclave with an inner volume of 30 ml. The bombs were heated at 120 °C for 5 days. The products consist of yellow square platelets with lengths of up to 1.5 mm. The yield of both compounds was 50% based on Mn.

Alternatively the products could be prepared under dynamic conditions. Stirring the mixtures of elemental Mn (0.055 g, 1 mmol), Sb (0.122 g, 1 mmol) and S (0.08 g, 2.5 mmol) with 2 ml aqueous amine solution in a teflon lined steel autoclave with an inner volume of 7 ml at 120 °C we obtained a microcrystalline powder of high purity and a yield of 80%. Under these conditions the reaction time is reduced from several days to few hours. But to obtain crystals which are suitable for single crystal X-ray work static conditions are necessary.

Structure refinement details

The intensity data were collected using a PHILIPS four-circle diffractometer in case of $Mn_2(MDAP)Sb_2S_5$ and a STOE Imaging Plate Diffraction System (IPDS I) in case of $Mn_2(DIEN)Sb_2S_5$ using graphite monochromated Mo-K_α radiation ($\lambda = 0.71073$ Å). The crystal of $Mn_2(DIEN)Sb_2S_5$ was non merohedrically twinned, and therefore both components were indexed and integrated separetely. The structures were solved using SHELXS-97 [40] and structure refinements were done on F^2 with SHELXL-97 [41]. All non-

Table 3. Atomic coordinates for $Mn_2(DIEN)Sb_2S_5$. Estimated standard deviations are given in parentheses. All atoms occupy the Wyckoff site 4e.

atom	*x*	*y*	*z*	U_{eq} [Å^2]
Sb(1)	0.3297(1)	0.4825(1)	0.2297(1)	0.018(1)
Sb(2)	0.3183(1)	0.7840(1)	0.2335(1)	0.019(1)
Mn(1)	0.6472(1)	0.6859(1)	0.2429(1)	0.025(1)
Mn(2)	0.4882(1)	0.6420(1)	0.5002(1)	0.020(1)
S(1)	0.5519(1)	0.7899(1)	0.3778(1)	0.019(1)
S(2)	0.5672(1)	0.5029(1)	0.3670(1)	0.019(1)
S(3)	0.2444(1)	0.6292(1)	0.3254(1)	0.020(1)
S(4)	0.7303(1)	0.8482(1)	0.1556(1)	0.020(1)
S(5)	0.3883(1)	0.6984(1)	0.0881(1)	0.020(1)
N(1)	0.6740(5)	0.5582(3)	0.1279(3)	0.031(1)
C(1)	0.8227(6)	0.5263(4)	0.1604(5)	0.040(1)
C(2)	0.8924(5)	0.5349(3)	0.2914(5)	0.032(1)
N(2)	0.8758(4)	0.6409(2)	0.3318(3)	0.026(1)
C(3)	0.9456(6)	0.6502(4)	0.4598(4)	0.035(1)
C(4)	0.9427(6)	0.7618(4)	0.5026(5)	0.040(1)
N(3)	1.0090(7)	0.8381(5)	0.4524(5)	0.060(1)

The U_{eq} is defined as one third of the trace of the orthogonalised U_{ij} tensor.

hydrogen atoms were refined with anisotropic displacement parameters. The H atoms were positioned with idealised geometry and refined with fixed isotropic displacement parameters applying a riding model with the parameters $d_{C-H} = 0.97$ Å and $d_{N-H} = 0.90$ Å. Both compounds are isostructural and crystallise in the monoclinic space group $P2_1/c$. The details of data acquisition and some refinement results are listed in Table 1, the atomic parameters of the compounds are listed in Tables 2 and 3.

Crystallographic data (excluding structure factors) for the structures reported in this paper have been deposited with the Cambridge Crystallographic Data Centre as supplementary publication no. CCDC 236008 for $Mn_2(MDAP)Sb_2S_5$ and CCDC 236009 for $Mn_2(DIEN)Sb_2S_5$. Copies of the data can be obtained, free of charge, on application to CCDC, 12 Union Road, Cambridge CB2 1EZ, UK. (fax: +44-(0)1223-336033 or email: deposit@ccdc.cam.ac.uk).

X-ray powder diffractometry

The X-ray powder patterns were recorded with a Siemens D5000 (Cu-K_α radiation, $\lambda = 1.54056$ Å) in Bragg-Brentano geometry.

Thermal analysis

The thermal measurements were performed using a Netzsch STA 429 DTA-TG device. The samples were heated in Al_2O_3 crucibles with a rate of 3 °C min^{-1} up to 400 respective 600 °C and purged in an argon stream of approximately 50 ml min^{-1}.

Magnetic measurements

Magnetic susceptibility measurements were conducted in a SQUID (Quantum Design) applying 1 T as external field. All experiments were performed in the zero field cooled mode followed by a field cooled run. The raw data were corrected for the core diamagnetism.

Table 4. Selected bond lengths for $Mn_2(DIEN)Sb_2S_5$ and $Mn_2(MDAP)Sb_2S_5$. Estimated standard deviations are given in parentheses.

$Mn_2(DIEN)Sb_2S_5$					
Sb(1) -	S(2)	2.4320(11)	Sb(1) -	S(3)	2.5133(9)
Sb(1) -	S(4)	2.4171(9)	Sb(2) -	S(1)	2.4198(11)
Sb(2) -	S(3)	2.5097(9)	Sb(2) -	S(5)	2.3832(9)
Mn(1) -	N(1)	2.224(4)	Mn(1) -	N(2)	2.277(4)
Mn(1) -	S(1)	2.5454(11)	Mn(1) -	S(2)	3.0393(1)
Mn(1) -	S(4)	2.5998(11)	Mn(1) -	S(5)	2.6619(12)
Mn(2) -	S(1)	2.6192(10)	Mn(2) -	S(2)	2.7041(10)
Mn(2) -	S(2)	2.6405(10)	Mn(2) -	S(3)	2.6566(13)
Mn(2) -	S(4)	2.5384(13)	Mn(2) -	S(5)	2.6608(10)
$Mn_2(MDAP)Sb_2S_5$					
Sb(1) -	S(2)	2.433(2)	Sb(1) -	S(3)	2.503(2)
Sb(1) -	S(4)	2.439(2)	Sb(2) -	S(5)	2.390(2)
Sb(2) -	S(1)	2.419(2)	Sb(2) -	S(3)	2.518(2)
Mn(1) -	N(1)	2.215(5)	Mn(1) -	N(2)	2.253(5)
Mn(1) -	S(1)	2.575(2)	Mn(1) -	S(2)	3.185(2)
Mn(1) -	S(4)	2.549(2)	Mn(1) -	S(5)	2.643(2)
Mn(2) -	S(1)	2.613(2)	Mn(2) -	S(2)	2.633(2)
Mn(2) -	S(2)	2.709(2)	Mn(2) -	S(3)	2.654(2)
Mn(2) -	S(4)	2.554(2)	Mn(2) -	S(5)	2.668(2)

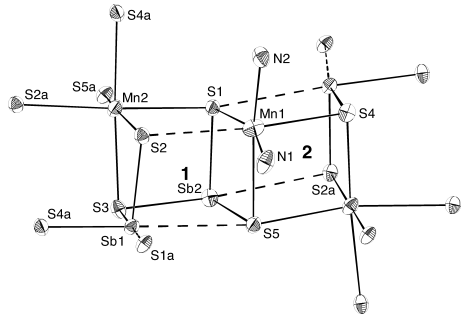

Fig. 1. The primary builing units $Mn(2)S_6$, $Mn(1)S_4N_2$ and the SbS_3 pyramids forming the two hetero-cubane units 1 and 2 (details see text). The ellidsoids are drawn at the 50% probability level. Note: Atoms labelled with an a are generated by symmetry.

Results and Discussion

The crystal structure

The two compounds $Mn_2(MDAP)Sb_2S_5$ and $Mn_2(DIEN)Sb_2S_5$ are new members of a series of polymeric manganese thioantimonates(III). They are isotypic to the previously reported compounds $Mn_2(L)Sb_2S_5$ with L = methylamine (MA), ethylamine (EA) and 1,3-diaminopropane (DAP) [15, 30]. The neutral framework is composed of MnS_6 and MnS_4N_2 octahedra and trigonal pyramidal SbS_3 units (see Fig. 1).

Amine	MA	EA	DIEN	DAP	MDAP
a [Å]	9.326(2)	10.618(5)	10.1859(7)	10.664(2)	10.669(7)
b [Å]	12.443(2)	12.457(5)	12.7806(6)	12.732(3)	12.805(2)
c [Å]	12.167(2)	12.185(3)	12.1256(8)	12.008(2)	12.072(1)
β [°]	107.82(2)	106.07(6)	110.173(8)	116.57(3)	115.786(7)
d(100) [Å]	8.879(3)	10.203(4)	9.561(7)	9.520(3)	9.607(7)
Cell volume [Å^3]	1344.2(2)	1551.0(2)	1481.7(2)	1455.5(2)	1485.1(4)
Density [g/cm^3]	2.845	2.568	2.765	2.682	2.692
non-H-Vol. [Å^3]	25.8	25.8	23.2	26.0	24.8

Table 5. Selected crystal data for the compounds $Mn_2(L)Sb_2S_5$. Estimated standard deviations are given in parentheses. Data for L = MA and DAP are taken from [15] and those for L = EA from [30].

Amine	MA	EA	DIEN	DAP	MDAP
Average Sb-S	2.454 Å	2.444 Å	2.446 Å	2.448 Å	2.450 Å
Sb1-S5	3.321(2) Å	3.299(1) Å	3.410(1) Å	3.391(2) Å	3.394(2) Å
Sb1-S1	3.128(2) Å	3.173(4) Å	3.209(4) Å	3.180(2) Å	3.361(3) Å
Sb2-S2	3.357(9) Å	3.348(3) Å	3.416(3) Å	3.392(2) Å	3.193(4) Å
Average Mn(2)-S	2.637 Å	2.634 Å	2.637 Å	2.634 Å	2.639 Å
Average Mn(1)-S[a]	2.643 Å	2.614 Å	2.604 Å	2.595 Å	2.593 Å
Mn(1)-S(2)	2.866(2) Å	2.927(1) Å	3.038(1) Å	3.074(2) Å	3.185(2) Å
Average Mn(1)-N	2.238 Å	2.238 Å	2.254 Å	2.214 Å	2.234 Å
N-Mn(1)-N	98.7(2)°	95.1(2)°	77.6(2)°	89.9(2)°	89.4(5)°
D1 (Mn2-Mn2)	8.716(3) Å	8.760(4) Å	9.153(1) Å	9.079(3) Å	9.138(3) Å
D2 (Sb1-Sb1)	7.696(3) Å	7.700(4) Å	7.522(1) Å	7.527(3) Å	7.513(3) Å
Ratio D1/D2	1.133	1.138	1.217	1.206	1.216

Table 6. Selected distances and angles for the compounds $Mn_2(L)Sb_2S_5$. Estimated standard deviations are given in parentheses. Data for L = MA and DAP are taken from [15] and those for L = EA from [30].

[a] The average Mn(1)-S bond lengths are calculated without the long Mn(1)-S(2) distance.

These units may be viewed as the primary building units (PBU). The short Sb-S distances (Table 4) as well as the S-Sb-S angles for both Sb centres are in the range reported in the literature for thioantimonates(III) [11 – 38].

Taking into account Sb-S distances up to the van der Waals radii of the two atoms (3.8 Å) the PBU's are interconnected in a way that hetero-cubane like moieties with composition $Mn_2Sb_2S_4$ are formed (see Fig. 1 the hetero-cubane marked as **1)**. These hetero-cubanes may be denoted as the secondary building units (SBU). Two edges of the cube are built by the relatively long Sb(1)-S(1) and Sb(2)-S(2) bonds (see Table 6 and Fig. 1). The interconnection of the SBU's generates a second hetero-cubane which is denoted as **2** in Fig. 1. In this cube one edge is formed by a long Sb(1)-S(5) contact and another edge by the relatively long Mn(1)-S(2) distance (Table 4). With the $6s^2$ lone pair of Sb(III) the environment of Sb(1) may be described as ψ-octahedral and that of Sb(2) as ψ-trigonal bipyramidal. The average Mn(2)-S distances as well as the Mn(1)-N bond lengths of the two compounds are in the range observed for the other members of the series (Tables 4 and 6). The most prominent changes around the two Mn atoms are discussed below.

The two different SBU's are joined *via* common faces, edges, and corners thus leading to the formation of layers within the (100) plane that contain ellipsoidal holes (Fig. 2). The layers are stacked onto each other

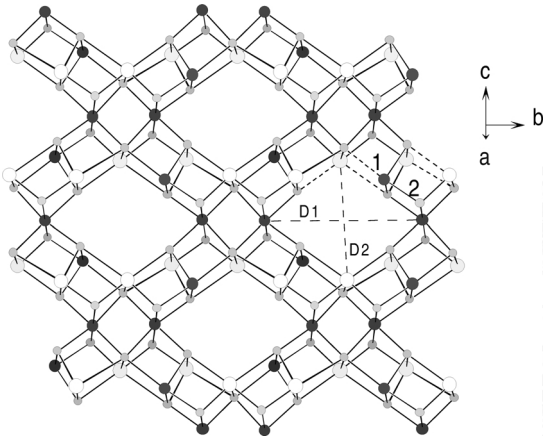

Fig. 2. Interconnection of the two hetero-cubane units yielding the layered $Mn_2Sb_2S_5$ framework. D1 and D2 are the two diameters of the ellipsoidal pores. Open circles: Sb; light grey circles: S; dark grey: Mn.

in a way that channels along [100] are formed. The amino ligands are directed into the ellipsoidal holes within the layers as well as perpendicular to the layers separating the sheets from each other (Fig. 3). The interactions between the layers are restricted to van der Waals bonds, but weak interlayer hydrogen bonding may also stabilise the framework. Interestingly, only two of the three N atoms of DIEN are bound to manganese and the third N atom is directed out of the layer plane. The normal displacement parameters for the N atom supports the assumption that at least in this com-

pound hydrogen bonding plays a non negligible role (d(N3-S5) = 3.67 Å with d(H4-S5) = 2.86 Å).

A) Influence of the amines onto the lattice parameters

The amines influence only moderately the *b* and *c* axes (see Table 5). But the *a* axis exhibits a significant increase with the size of the amines. From the smallest amine MA to the largest amine MDAP the *a* axis is enlarged by 1.34 Å. A pronounced effect onto the monoclinic angle is observed which is caused by the special arrangement of the ligands that point into the interlayer space. The monodentate amines between the layers are arranged in a "head-to-head" fashion and it is obvious that the larger C_2H_5 group of EA requires more space than the CH_3 group of MA. In contrast, the bidentate amines of one layer point into pockets formed by the amines of the neighboured layer. To achieve such an arrangement the layers must "slip" relative to each other and the monoclinic angle is enhanced. The different arrangements are depicted in Fig. 3 for EA and DAP as examples. As a consequence of the arrangement of the amines, the interlayer distances d(100) do not follow the simple trend of the *a* axis (Table 5). Further consequences of the special ordering are smaller unit cell volumes as well as higher densities for DIEN, DAP and MDAP compared to the EA compound (see Table 5). But the most dense compound is $Mn_2(MA)_2Sb_2S_5$ reflecting the space requirements of the H atoms bound to carbon in DIEN, DAP and MDAP.

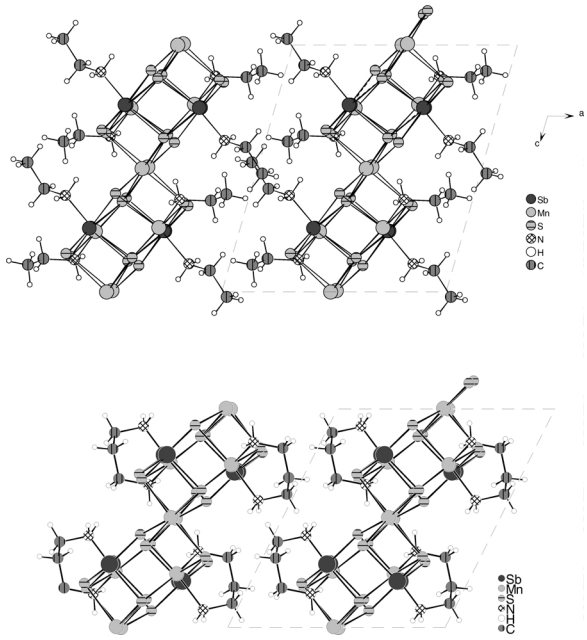

Fig. 3. Arrangement of the layers with view along the b axis for $Mn_2(EA)_2Sb_2S_5$ (top) and $Mn_2(DAP)Sb_2S_5$ (bottom). Note that the view direction is identical for both structures.

B) Influence of the amines onto the geometry of the framework

The short Sb-S bonds, the average Mn(1)-N as well as the average Mn(2)-S distances show no pronounced and systematic alterations within the series (Table 6). The Mn(2)-S bond lengths are in accordance with the sum of the ionic radii of Mn^{2+} and S^{2-} [42]. The relatively long Sb(1)-S(5) and Sb(1)-S(1) separations are slightly longer for the bidentate amines.

The strongest changes are found for the Mn(1)-S bonds and the angles N-Mn(1)-N (Table 6). Three of the four Mn(1)-S distances are in the usual range whereas one separation is significantly larger (see also Table 4). The Mn(1)-S(2) distance increases from 2.866(2) Å for L = MA up to 3.185(2) Å for L = MDAP, *i.e.* by 0.319 Å (Table 6). This elongation reduces the Coulomb interaction between Mn^{2+} and S^{2-} and the shielding of the positive charge located on the Mn ion becomes weaker with increasing Mn(1)-S(2) separation. As a counteracting effect the average Mn(1)-S bond lengths to the remaining three S ions become shorter and decrease from 2.643 (MA) to 2.593 (MDAP).

For the two monodentate amines the N-Mn-N angles are 98.7° (MA) and 95.1° (EA). The two bidentate amines DAP and MDAP form six membered rings MnN_2C_3 with a chair conformation and N-Mn-N angles being fixed near 90° by conformational requirements (see Table 6). A strong deviation from 90° is observed for L = DIEN because a five membered ring MnN_2C_2 is formed that forces an acute angle of 77.6° (see Table 6).

The reason why the Mn(1)-S(2) distance is significantly larger than the other Mn-S bonds may be due to the fact that the S(2) atom is bound to three Mn^{2+} ions (2×Mn(2), Mn(1)) and two Sb(III) ions. All other S atoms have bonds to one Mn^{2+} and two Sb(III) (S(3)) or to two Mn^{2+} and two Sb(III) ions. It is reasonable that two medium long Mn-S(2) distances are energetically less favourable than one short and one long bond. In addition, different sterical and spatial requirements as well as the different bonding properties of the amino-ligands bound to Mn(1) are altered going from MA to MDAP further weakening the Mn(1)-

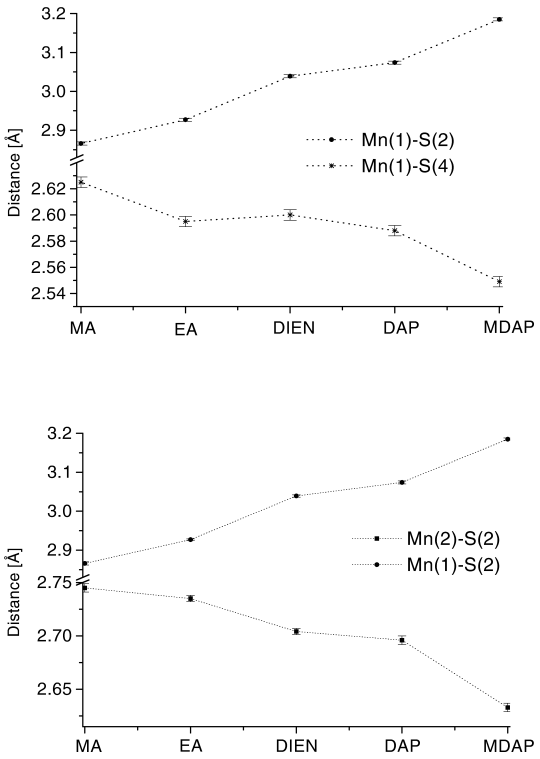

Fig. 4. Change of the Mn(1)-S(2)/Mn(1)-S(4) (top) and of Mn(1)-S(2)/Mn(2)-S(2) (bottom) bond lengths as function of the amine. Vertical bars represent the estimated standard deviations and the dotted lines serve as guides for the eyes.

S(2) bonding interactions. Simultaneously, the lengthening of the Mn(1)-S(2) distances is accompanied by a strengthening of the *trans* Mn(1)-S(4) bond (see Fig. 4, top). In summary, the Mn(1)-S(2) bonding interaction is the "weakest" link within the network allowing the crystal structure to relax and to reduce an internal "strain" exerted by the amino ligands. The drastic change of the Mn(1)-S(2) bond length also influences the environment of the Mn(2) atom. As an example the alteration of the Mn(2)-S(2) bond is displayed in Fig. 4 (bottom). The strong elongation of the Mn(1)-S(2) distances leads to a shortening of the Mn(2)-S(2) bond lengths.

As noted above the interconnection of the different building blocks yields ellipsoidal pores that are filled by the amines. The diameters D1 (Mn(2) - Mn(2)) and D2 (Sb(1) - Sb(1)) (see Fig. 2) give an impression of the changes of the shape of the rings caused by the different amines. D1 increases from 8.72 Å for MA to 9.15 Å for DIEN (see Table 6). Simultaneously D2 slightly decreases. The ratio D1/D2 reveals that for the bidentate amines the pores deviate stronger from an ideal round hole.

C) The syntheses

With respect to the reactions under solvothermal conditions some surprising results should be highlighted here.

I) Despite a 60fold excess of the amines with respect to the amount of Mn only one of the two Mn atoms is bound to the N atoms of the amines and the second Mn atom is exclusively in an octahedral environment of 6 S atoms.

II) Manganese forms very stable complexes with chelating ligands like DAP, MDAP, and DIEN. Hence it is surprising that no isolated complexes are built as for instance when Ni or Co are used as the transition metals under comparable conditions. A remarkable difference between Mn^{2+} and Co^{2+}/Ni^{2+} is the polarisability of the cations. Within the framework of the HSAB concept Mn^{2+} prefers the softer S^{2-} ions whereas the harder Co^{2+}/Ni^{2+} ions have a preference for the N atom. Nevertheless, such simple considerations do not explain the different behaviour of the two independent Mn^{2+} ions in the $Mn_2(L)Sb_2S_5$ compounds.

III) The amine DIEN has three amino groups that can coordinate to the Mn^{2+} ions. In principle one would expect the formation of an octahedral $[Mn(DIEN)_2]^{2+}$ complex ion. But in the polymeric network only two N atoms act as ligands and the third N atom seems to be "superfluous" for the formation of the structure.

D) Thermal stability

The thermal properties of the two new compounds were investigated using difference thermal analysis (DTA) and thermogravimetry (TG) performed under an argon atmosphere. Both compounds start to decompose at about 275 °C with accompanying endothermic signals in the DTA curves at $T_{onset} = 250$ °C (DIEN) and $T_{onset} = 275$ °C (MDAP). For both compounds a one step decomposition is observed with a weight loss of 12.5% ($\Delta m_{theo} = 14.6\%$) for $Mn_2(MDAP)Sb_2S_5$ and 17.1% ($\Delta m_{theo} = 16.7\%$) for $Mn_2(DIEN)Sb_2S_5$. At 594 °C the melting point of the decomposition product Sb_2S_3 could be observed. In the X-ray powder patterns of the dark grey residues MnS and Sb_2S_3 could be identified. The thermal stability of the three other compounds was also investigated. The sample with L =

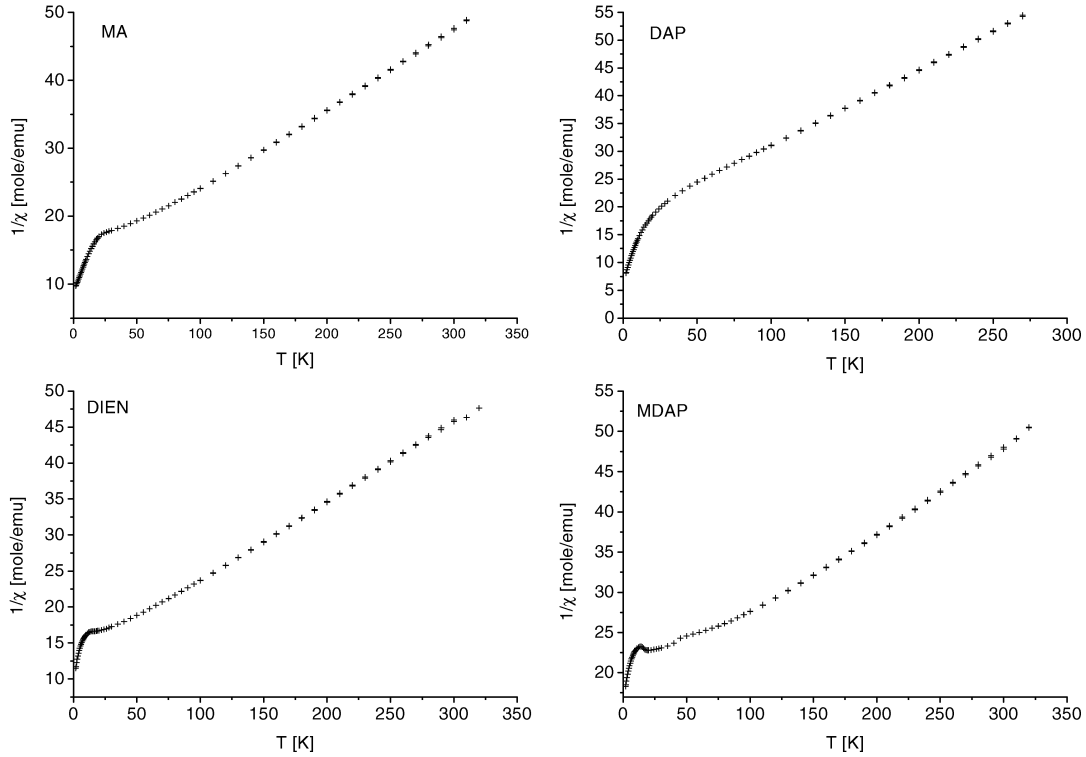

Fig. 5. Temperature dependence of the inverse magnetic susceptibilities for $Mn_2(L)Sb_2S_5$.

DAP shows also only one step in the TG curve with $T_{onset} = 268$ °C and a weight loss of 11.8% ($\Delta m_{theo} = 12.8\%$). The two compounds with MA and EA are less stable and both show a two step decomposition with signals in the DTA curve located at $T_{onset} = 175$ and 250 °C (MA) and $T_{onset} = 195$ and 225 °C (EA). The weight loss for MA is 8.6% ($\Delta m_{theo} = 10.8\%$) and 13.0% ($\Delta m_{theo} = 14.9\%$) for EA.

E) Magnetic properties

The inverse magnetic susceptibilities of $Mn_2(L)Sb_2S_5$ (L = MA, DAP, DIEN and MDAP) are displayed in Fig. 5. Below a distinct temperature the experimental data deviate from straight lines passing a more or less pronounced maximum and finally drop again. The curves are reminiscent for low-dimensional antiferromagnetic systems. The evaluation of the data with the Curie-Weiss law yields an effective magnetic moment of about 5.90 μ_B/Mn^{2+} for all compounds which is in accordance with the spin only value of the d^5 electronic configuration. The Weiss constant Θ amounts to −105.1(5), −110.8(7), −127.3(6), and −142.2(2) K for L = MA, DIEN, DAP and MDAP respectively. For all compounds the large negative value of Θ indicates strong antiferromagnetic exchange interactions, and the strength increases from MA to MDAP. The Mn-Mn separations (3.638 Å for L = DIEN; 3.673 for L = MDAP) are too long for direct magnetic exchange and hence a superexchange must be considered. All Mn-S-Mn angles are near 90° and according to the Goodenough-Kanamori rules ferromagnetic superexchange can be expected. It can be assumed that

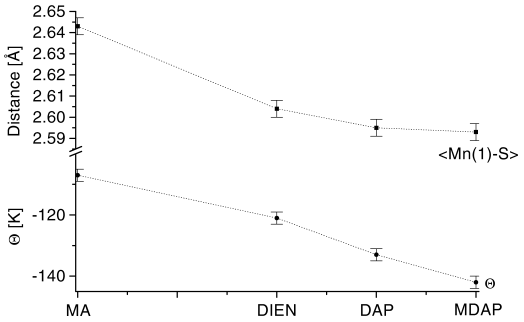

Fig. 6. Evolution of the average Mn(1)-S bond lengths and of the Weiss constant Θ. The plot should demonstrate how the amine influences the $\langle Mn(1)\text{-}S\rangle$ distance and as a consequence the value for the Weiss constant. Note that the average Mn(1)-S distance was calculated neglecting the long Mn(1)-S(2) bond. The dotted lines serve only as guide for the eyes.

coupling across the layers is very weak and one possible explanation for the experimentally observed antiferromagnetic exchange is an antiferromagnetic arrangement of neighboured ferromagnetic layers.

Analysing the structural details a strong correlation between the Mn(1)-S bond lengths and the evolution of Θ becomes obvious (Fig. 6). Neglecting the long Mn(1)-S(2) bonds the average Mn(1)-S bonds of the remaining Mn(1)-S distances decrease from MA to MDAP which strengthen the superexchange interactions. In addition, several Mn(2)-S distances are also shortened across the series of compounds (see for instance Fig. 4, bottom) which may also make the exchange interactions more effective, and finally slight changes of the actual Mn-S-Mn angles must also be taken into account.

Acknowledgements

This work has been supported by the State of Schleswig-Holstein and the Deutsche Forschungsgemeinschaft.

[1] H. A. Graf, H. Schäfer, Z. Naturforsch. **27b**, 735 (1972).
[2] G. Dittmar, H. Schäfer, Z. Anorg. Allg. Chem. **437**, 183 (1977).
[3] G. Dittmar, H. Schäfer, Z. Anorg. Allg. Chem. **414**, 211 (1975).
[4] G. Dittmar, H. Schäfer, Z. Anorg. Allg. Chem. **441**, 93 (1978).
[5] G. Dittmar, H. Schäfer, Z. Anorg. Allg. Chem. **441**, 98 (1978).
[6] B. Eisenmann, H. Schäfer, Z. Naturforsch. **34b**, 383 (1979).
[7] G. Cordier, H. Schäfer, C. Schwidetzky, Z. Naturforsch. **39b**, 131 (1984).
[8] K. Volk, P. Bickert, R. Kolmer, H. Schäfer, Z. Naturforsch. **34b**, 380 (1979).
[9] G. Cordier, H. Schäfer, Rev. Chim. Miner. **18**, 218 (1981).
[10] G. Cordier, H. Schäfer, C. Schwidetzky, Rev. Chim. Miner. **22**, 722 (1985).
[11] M. Schaefer, L. Engelke, W. Bensch, Z. Anorg. Allg. Chem. **629**, 1912 (2003).
[12] M. Schaefer, C. Näther, W. Bensch, Solid State Sci. **5**, 1135 (2003).
[13] R. Kiebach, W. Bensch, R.-D. Hoffmann, R. Pöttgen, Z. Anorg. Allg. Chem. **629**, 532 (2003).
[14] R. Stähler, W. Bensch, Eur. J. Inorg. Chem. 3073 (2001).
[15] W. Bensch, M. Schur, Eur. J. Solid State Inorg. Chem. **33**, 1149 (1996).
[16] M. Schur, W. Bensch, Z. Naturforsch. **57b**, 1 (2002).
[17] W. Bensch, C. Näther, R. Stähler, Chem. Commun. 477 (2001).
[18] R. Stähler, C. Näther, W. Bensch, Eur. J. Inorg. Chem. 1835 (2001).
[19] R. Stähler, W. Bensch, Z. Anorg. Allg. Chem. **628**, 1657 (2002).
[20] R. Stähler, C. Näther, W. Bensch, Acta Crystallogr. **C57**, 26 (2001).
[21] X. Wang, F. Liebau, J. Solid State Chem. **111**, 385 (1994).
[22] A. V. Powell, R. Paniagua, P. Vaqueiro, A. M. Chippindale, Chem. Mater. **14**, 1220 (2002).
[23] A. V. Powell, S. Boissiere, A. M. Chippindale, J. Chem. Soc., Dalton Trans. 4192 (2000).
[24] A. Pfitzner, D. Kurowski, Z. Kristallogr. **215**, 373 (2000).
[25] A. V. Powell, S. Boissière, A. M. Chippindale, Chem. Mater. **12**, 182 (2000).
[26] W. S. Sheldrick, H.-J. Häusler, Z. Anorg. Allg. Chem. **557**, 195 (1988).
[27] R. Stähler, W. Bensch, J. Chem. Soc., Dalton Trans. 2518 (2001).
[28] V. Spetzler, H. Rijnberk, C. Näther, W. Bensch, Z. Anorg. Allg. Chem. **630**, 142 (2004).
[29] H.-O. Stephan, M. G. Kanatzidis, J. Am. Chem. Soc. **118**, 12226 (1996).
[30] M. Schur, C. Näther, W. Bensch Z. Naturforsch. **56b**, 79 (2001).
[31] X. Wang, A. J. Jacobson, F. Liebau, J. Solid State Chem. **140**, 387 (1998).
[32] Y. Ko, K. Tan, J. B. Parise, A. Darovsky, Chem. Mater. **8**, 493(1996).
[33] J. B. Parise, Y. Ko, Chem. Mater. **4**, 1446 (1992).
[34] M. Schur, A. Gruhl, C. Näther, I. Jess, W. Bensch, Z. Naturforsch. **54b**, 1524 (1999).
[35] R. Stähler, B.-D. Mosel, H. Eckert, W. Bensch, Angew. Chem. **114**, 4671 (2002).
[36] R. Stähler, C. Näther, W. Bensch, J. Solid State Chem. **174**, 264 (2003).
[37] L. Engelke, C. Näther, W. Bensch, Eur. J. Inorg. Chem. 2936 (2002).
[38] P. Vaqueiro, A. M. Chippindale, A. R. Cowley, A. V. Powell, Inorg. Chem. **42**, 7846 (2003).
[39] X. Wang, F. Liebau, Acta Crystallogr. **B52**, 7 (1996).
[40] G. M. Sheldrick, SHELXS-97, University of Göttingen (1997).
[41] G. M. Sheldrick, SHELXL-97, University of Göttingen (1997).
[42] R. D. Shannon, Acta Crystallogr. **A32**, 751 (1976).